Effect of Free-Stream Turbulence on the Aerodynamic Characteristics of a Circular Cylinder

Mikio ARIE* Masaru KIYA*
Yasuhiro SUZUKI* Hiroshi KOTO**

(Received June 30, 1978)

Abstract

The effect of free-stream turbulence of high intensity on the flow past a rigid circular cylinder was studied experimentally in a Reynolds-number range 1.1×10^4—4.1×10^4. A square-meshed grid was used to produce a homogeneous turbulent-flow field. The intensity and scale of the turbulent flow in which the cylinder was immersed were varied by positioning the cylinder at various locations downstream of the grid. Measurements were made on time-averaged pressure distributions around the cylinder, time-averaged drag coefficient, Strouhal number of the vortex shedding, spanwise correlation length and energy spectrum of the fluctuating longitudinal velocity component in the wake of the cylinder. These properties of flow around the cylinder were found to be fairly well correlated with the parameter $[(\overline{u'^2})^{1/2}/U_\infty]/(d/L_x)$, which was originally proposed by the authors. Here, $(\overline{u'^2})^{1/2}$ and L_x are the longitudinal turbulence intensity and scale of the flow surrounding the cylinder, U_∞ is its time-averaged velocity and d is the diameter of the cylinder.

1. Introduction

In recent years the need for more realistic design criteria for artificial structures on the ground has given rise to increasing attention on the prediction of the response of such structures to atmospheric turbulence. Since it would be unrealistic to perform fluctuating wind-loading tests on a complete building owing to the considerable amount of experimentation this would necessitate, it is desirable to devise a theoretical or empirical procedure to allow for this prediction. A development of such an approach, however, is hampered by our lack of understanding of some of the important flow phenomena involved in the interaction between the atmospheric turbulence and structures.

In order to be able to understand the actual interaction, it is important to clarify the effect of the free-stream turbulence on the aerodynamic characteristics of bluff bodies of relatively simple shapes. The object of this paper is to examine the relationship between the approaching turbulent flow and the time-averaged drag force, together with the characteristics of the shed vortices, on a series of circular cylinders set normal to the flow. The present paper is concentrated on

* Laboratory of Fluid Mechanics I, Department of Mechanical Engineering.
** Hitachi Cable Co. Ltd.

the effects of turbulence, excluding the discussion on the effects of mean shear. Although the model of the present study is a rather simple example of the problem, it retains important features of the interaction between turbulence and bluff bodies.

A few important concepts of a turbulent flow past bluff bodies will be briefly reviewed. Hunt[1] formulated a theory, based on the rapid distortion theory of Batchelor and Proudman[2], for the purpose of analysing the distortion of turbulence in a flow sweeping past a body. It is assumed in the rapid distortion theory that the mean flow is irrotational as well as $(\overline{u'^2})^{1/2}/U_\infty \ll 1$ and the neglect of viscous effects is justified if the distortion takes place in a short time so that the viscous decay of energy is very small. The rapid distortion theory applied to the turbulent flow sweeping past a body also requires

$$(\overline{u'^2})^{1/2}/U_\infty \ll L_x/d \tag{1}$$

where $(\overline{u'^2})^{1/2}$ is the root-mean-square value of longitudinal component of turbulence, U_∞ is the mean velocity, L_x is the integral length scale in the mean-flow direction of the longitudinal component of turbulence and d is a representative dimension of body. Bearman[3] described in terms of the entrainment mechanism the effect of turbulence on the mean and fluctuating forces acting on a square plate set normal to a turbulent stream. He showed that the mean and fluctuating forces and base pressure coefficient were correlated with a parameter $[(\overline{u'^2})^{1/2}/U_\infty]/(L_x^2/A)$, A being the area of the square plate. In order to find a relationship between the properties of free-stream turbulence and the critical Reynolds number concerned with the drag crisis of smooth bluff bodies such as a circular cylinder, Taylor[4] proposed a turbulence parameter, now called the Taylor number, in the form

$$T=\left[(\overline{u'^2})^{1/2}/U_\infty\right](d/L_x)^{1/5} \tag{2}$$

However, the present experimental investigation has shown that the turbulence parameters proposed by Bearman[3] and Taylor[4] are not sufficiently appropriate to interpret the effect of turbulence on both the aerodynamic characteristics of a circular cylinder and the statistical properties of the velocity fluctuation associated with the shed vortices. A more suitable parameter is found to be $\mathrm{Tu}=[(\overline{u'^2})^{1/2}/U_\infty] \times (d/L_x)$, which is suggested from Eq. (1).

2. Nomenclature

A	area of square flat plate
C_D	drag coefficient
C_p	pressure coefficient
C_{pb}	base-pressure coefficient
F	power spectrum density
L_x	longitudinal integral-length scale of turbulence
L_z	spanwise integral-length scale of shed vortices
M	mesh size of grid
N	energy of background turbulence

R Reynolds number or correlation coefficient
S energy at vortex-shedding frequency
S_t Strouhal number
T Taylor number
Tu turbulence parameter defined by Eq. (3)
U_∞ free-stream velocity
X, Y, Z coordinate system (see Fig. 1)
d diameter of circular cylinder
t time
u' fluctuating longitudinal velocity component
ζ separation between two hot-wire probes
τ time lag
θ angle measured from forward stagnation point of circular cylinder

3. Experimental arrangement

The experiments were conducted in an air tunnel 100 cm in length with a square cross-section of 30×30 cm. The tunnel is of a through-flow type, and the turbulence level of the free-stream was about 1% at the maximum velocity of 23 m/sec. A highly turbulent flow was generated by a square-meshed grid installed at the entrance of the working section. The grid was constructed from 15 mm × 15 mm wooden slats spanning the tunnel. The distance between the center of slats, i.e. the mesh size M, was 45 mm. With the grid in position, the maximum velocity of airflow in the tunnel was reduced to about 11 m/sec. The circular cylinders

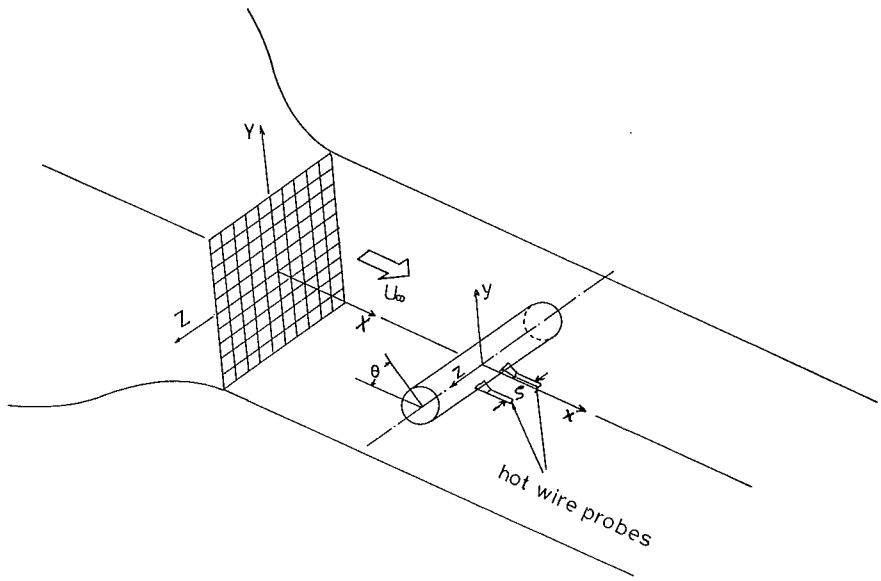

Fig. 1. Schematic representation of circular cylinder installed in position in air tunnel. The center of the cylinder is located at $X=300$ mm or 600 mm.

tested had a diameter of 15 mm, 30 mm and 60 mm respectively, each spanning the whole width of the test section. A pressure tap of 0.9 mm in diameter was drilled onto the surface of each cylinder at its mid-span position. The pressure on the circular cylinders were measured by a Betz-type manometer. The pressure distributions thus obtained were intergrated to yield the drag force acting on the cylinders. Turbulence measurements were made with KANOMAX 2100 constant-temperature type of hot-wire anemometer. Statistical characteristics of the fluctuating velocities were obtained by means of the SAI-42A real-time digital correlator and SAI-470 digital Fourier transformer. The coordinate system and the definition of main symbols are shown in Fig. 1.

4. Results and discussion

4.1. Characteristics of the turbulence generated by grid

The variation of the intensity $(\overline{u'^2})^{1/2}/U_\infty$ and the longitudinal integral length scale L_x of the streamwise component of turbulence, along the center-line of the working section, is shown in figure 2. The mean velocity and the intensity of turbulence are found to be uniform within the deviations of $\pm 3\%$ and $\pm 2\%$, respectively, over a range of $-40\ \text{mm} \leqq Y \leqq 40\ \text{mm}$ and $-70\ \text{mm} \leqq Z \leqq 70\ \text{mm}$ at the

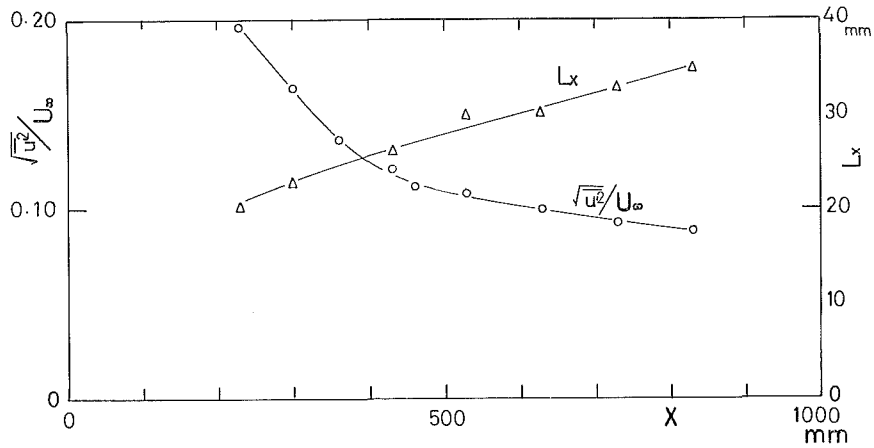

Fig. 2. Variation of intensity and scale of streamwise component of turbulence along ceter-line of working section.

TABLE 1. Summary of experimental conditions and main results

Case	d (mm)	$(\overline{u'^2})^{1/2}/U_\infty$	L_x/d	R ($\times 10^4$)	C_D	$-C_{pb}$	S_t	$(L_x/d)_{\theta=90°}$	Tu
1	15	0.102	2.0	1.1	1.105	0.98	0.188	1.87	0.051
2	30	0.102	1.0	2.1	—	—	0.197	1.47	0.102
3	60	0.102	0.5	4.1	0.890	0.88	0.210	0.61	0.204
4	15	0.164	1.51	1.1	1.053	0.81	0.184	1.06	0.109
5	30	0.164	0.76	2.1	—	—	0.200	0.51	0.216
6	60	0.164	0.38	4.1	0.487	0.49	0.258	0.30	0.432

sections where the test cylinders are to be installed. The longitudinal integral length scale L_x can be calculated from

$$L_x = U_\infty \int_0^\infty R_{u'}(\tau)\, d\tau$$

where $R_{u'}(\tau)$ is the autocorrelation coefficient of turbulence defined by

$$R_{u'}(\tau) = \overline{u'(t)\, u'(t+\tau)} / [\overline{u'(t)}]^2$$

An over-bar in this equation implies the time averaging and τ is the time lag. Table 1 summarizes the results of turbulence properties and some other important parameters obtained in the present experiments.

4.2. Pressure distribution and drag coefficient

Measured pressure distributions are shown in Fig. 3 plotted against a reference

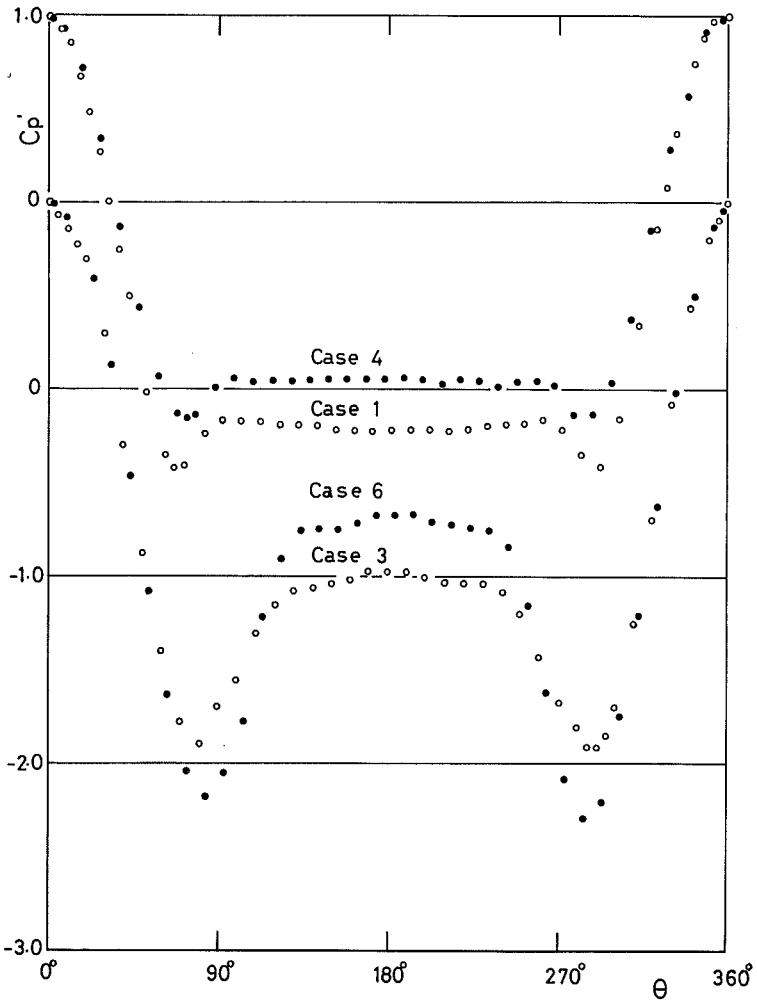

Fig. 3. Time-averaged pressure distribution around circular cylinder.

angle θ. In these measurements the Reynolds number based on the diameter of the cylinder is varied from 1.1×10^4 to 4.1×10^4. No attempt was made to correct the measured pressures for the turbulence intensity or any errors associated with turbulence effects (see Hinze[5]).

Since the blockage ratio d/h, where d is the diameter of the cylinder and h is the height of the working section, amounts to 20%, it is necessary to correct the experimental results because of the wall-interference effect. For this purpose use is made of the empirical formulas of Allen and Vincenti,[6] which give the corrected values of velocity and drag coefficient, U_∞ and C_D, in terms of the measured values U'_∞ and C'_D:

$$\frac{U_\infty}{U'_\infty}=1+\frac{1}{4}C'_D\left(\frac{d}{h}\right)+0.82\left(\frac{d}{h}\right)^2$$

$$\frac{C_D}{C'_D}=1-\frac{1}{2}C'_D\left(\frac{d}{h}\right)-2.5\left(\frac{d}{h}\right)^2$$

When the corrected values of pressure coefficient C_p are needed, they can be evaluated from

$$(C_p-1)=\left(\frac{U'_\infty}{U_\infty}\right)^2(C'_P-1)$$

where C'_p is the pressure coefficient before correction. Reynolds number and Strouhal number can also be corrected in the same manner as the velocity U_∞. It should be noted that the maximum corrections to the mean velocity U'_∞, drag coefficient C'_D and base pressure coefficient C'_{pb} were about 6.2%, 16% and 39%, respectively.

As is tabulated in Table 1, the pressure distributions in Fig. 3 show the experimental results for two sets of different diameters of cylinder and turbulence. The order of Reynolds number is 10^4 in all the four cases. Comparison of pressure distributions between cases 1 and 4 or 3 and 6 for respectively the same size of cylinder clearly shows that a significant difference of the base pressure acting on the cylinders results from the turbulence intensity and scale included in the oncoming flow. It is usually difficult to exactly detect the position of separation point based on the pressure-distribution curve of a cylinder. However, Fig. 3 seems to show that the separation points are slightly shifted toward the rear side with an increase of the turbulence intensity. The base pressure coefficient C_{pb} and the drag coefficient C_D were determined from the measured pressure distributions. C_{pb} was estimated from the average value of the pressure coefficient in the region between $\theta=130°$ and 230°, where the pressure distributions were almost uniform. As previously explained, C_D was calculated by integrating the pressure distribution along the cylinder surface. Neither Bearman's turbulence parameter nor Taylor number can successfully by applied to correlate the values of C_D and C_{pb} obtained for various combinations of cylinder diameter and turbulence properties. After some attempts, the following turbulence parameter Tu was found to be an appropriate one:

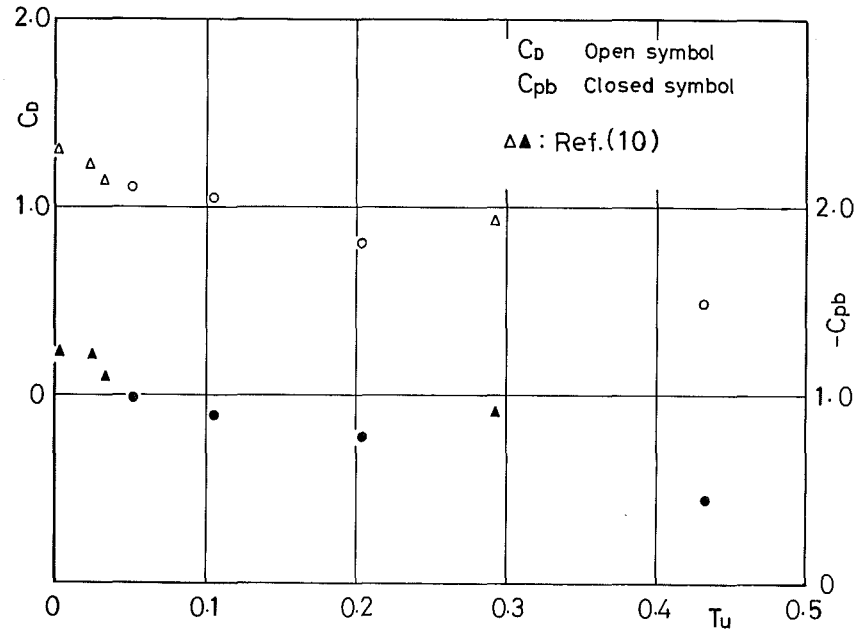

Fig. 4. Drag coefficient and base pressure coefficient versus turbulence parameter Tu.

$$Tu=\left[(\overline{u'^2})^{1/2}/U_\infty\right]/(d/L_x) \qquad (3)$$

Figure 4 shows C_D and $-C_{pb}$ as functions of the newly proposed turbulence parameter Tu. It seems that fairly good correlations are obtained by the employment of this parameter.

4.3. Spanwise correlation

For the purpose of estimating the magnitude of the fluctuating lift acting on a certain length of cylinder, it is important to obtain the variation of correlation between the local lifts simultaneously measured at two stations by changing the

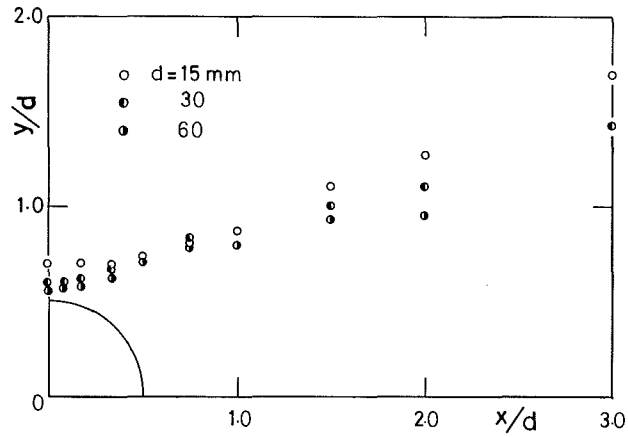

Fig. 5. Position of hot-wires for measurement of correlation and spectra.

distance between the stations. The correlation coefficients approach zero as the distance between two stations becomes large. The main reason for the decay of the correlation coefficient is the lack of two-dimensionality of the shed vortices. A measure of the spanwise uniformity of the vortices can be obtained by correlating the outputs of two hot-wires displaced along a line parallel to the cylinder axis. The hot-wires must be positioned far enough away from the cylinder surface to avoid turbulence within the shear layer which convects over the probe but near enough to ensure a strong shedding signal. The positions of correlation measurements are shown in Fig. 5. Even if the positions of the probes were removed slightly in the vertical y direction maintaining the x coordinate constant, insignificant changes were obtained in the resulting correlation curves.

The spanwise correlation length L_z of the shed vortices is defined as the area beneath the correlation curve, i. e.

$$L_z = \int_0^\infty R_{u'u'}(\zeta)\, d\zeta$$

where $R_{u'u'}(\zeta)$ is the spanwise correlation of longitudinal turbulence component

$$R_{u'u'}(\zeta) = \overline{u'(z)\, u'(z+\zeta)} / \overline{u'(z)^2}$$

and ζ is the distance between the probes.

At any instant the shed votex sheets will not extend over the whole length of the cylinder; it appears that the average coherent length of the shed vortex sheets is about several times the cylinder diameter. Bearman and Wadcock[7] me-

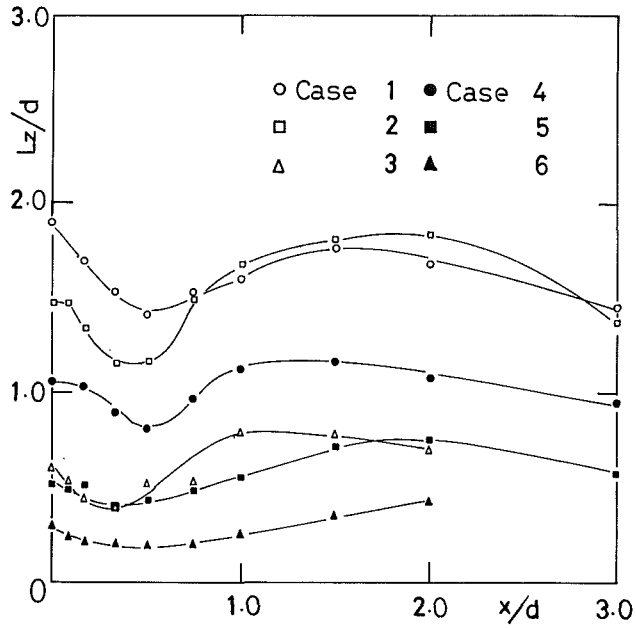

Fig. 6. Variations of spanwise correlation length of shed vortices in downstream direction.

asured the correlation length for a circular cylinder immersed in a relatively smooth flow. They found the value to be 3.7 times the diameter at a Reynolds number of 2.5×10^4. El Baroudi[8] also measured the correlation length in a Reynolds number range of $10^4-4.5\times10^4$ with hot-wire probes at 90° points of a circular cylinder. His measurements yielded rather larger correlation lengths than Bearman and Wadcock's result. The variation of the correlation length L_z with the downstream distance is presented in Fig. 6.

A careful examination of Fig. 6 reveals two important aspects of the spanwise correlation length. Firstly, the general level of the correlation length decreases as the free-stream turbulence intensity increases. Secondly, the $L_z/d\sim x/d$ curves exhibit complicated shapes which attain a maximum at $x/d\fallingdotseq0$, a minimum at $x/d\fallingdotseq0.5$ and another maximum in the range $1.0<x/d<2.0$.

It is worthwhile to mention that the minima of the correlation length invariably appear at $x/d\fallingdotseq0.5$ irrespective of the turbulence intensity and scale, as far as the present experiment is concerned. The location somewhere in a range of $1<x/d<2$, at which the correlation length attains a maximum, approximately corresponds to the end of the formation region of vortices measured by Bloor[9] at a Reynolds number of 10^4. Fourier transform of the autocorrelation of a hot-wire signal yields power spectra of the velocity fluctuation behind the cylinder. Figure 7 shows the correlation length at the 90° point ($x/d=0$) of the cylinder and the Strouhal number St of the vortex shedding as functions of the turbulence parameter Tu. Also indicated in Fig. 7 is the spanwise correlation length of the fluctuating surface

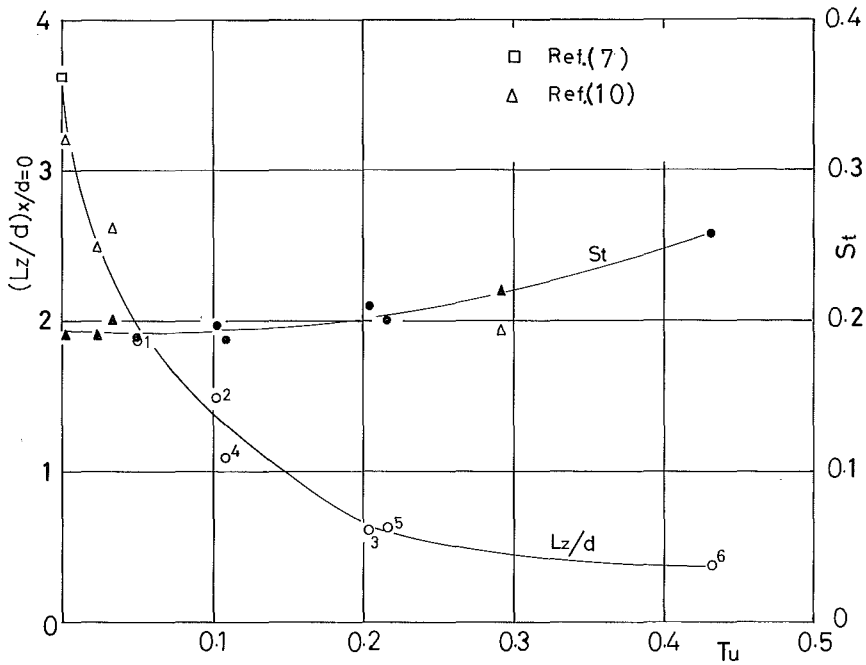

Fig. 7. Spanwise correlation length at $\theta=90°$ and Strouhal number versus turbulence parameter Tu.

pressure at the 90° point determined by Surry[10]. It is interesting to note that these data, except for one point of the correlation length measured by Surry, gather on single curves with fairly good accuracy.

The effects of turbulence on the shedding peak exist primarily in the broadening and lowering of the power spectrum as may be adjudged from the experimental results in Fig. 9. Although the effect of turbulence on Strouhal number is small, the present results show an increasing trend of St as Tu increases.

4.4. Energy of shed vortex

In the wake of the circular cylinder, a hot-wire signal shows a mixed periodic-random fluctuation. The periodic part of the signal corresponds to the shedding of vortices whereas the random part corresponds to the turbulent fluctuation which conceptually consists of the grid-generated turbulence and wake turbulence. Accordingly the variance $\overline{u'^2}$ of the velocity fluctuation, which will be simply called as the energy, can be partitioned into

$$\overline{u'^2} = \overline{u_n'^2} + \overline{u_s'^2}$$

where the suffixes n and s denote the contribution from the random part or noise and that from the periodic part, respectively. The energy of velocity fluctuation

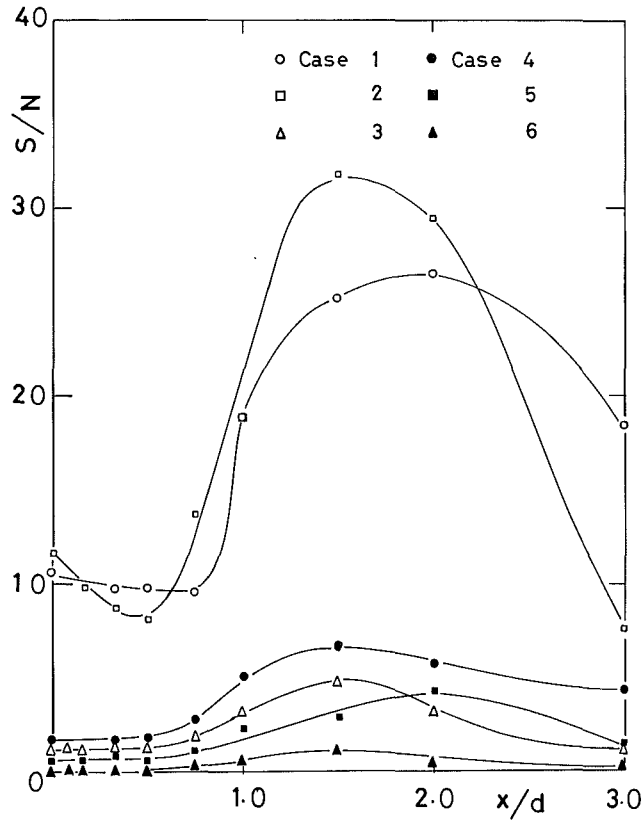

Fig. 8. Variation of energy at vortex-shedding frequency in downstream direction.

corresponding to the frequency of the vortex shedding n_s can be written as

$$\overline{[u'(n_s)]^2} = \overline{[u'_n(n_s)]^2} + \overline{[u'_s(n_s)]^2}$$

One now introduces the symbols

$$N = \overline{[u'_n(n_s)]^2}$$

$$S = \overline{[u'_s(n_s)]^2}$$

In order to assess the decay of strength of the periodic component in the turbulent free stream, one introduces the ratio S/N. Figure 8 shows the measured values of S/N plotted against the downstream distance x/d. When the free-stream turbulence level is relatively low (cases 1 and 2), the major part of the energy is concentrated at the shedding frequency n_s and it may be represented as a discrete part of the spectrum. As the turbulence level becomes higher, however, the background turbulence level exceeds the periodic signal so that little evidence of the shedding frequency remains (case 6). The general level of the S/N ratio decreases as the free-stream turbulence intensity increases. It is interesting to note that the S/N ratio for cases 1 and 2 shows qualitatively the same trend as the spanwise cor-

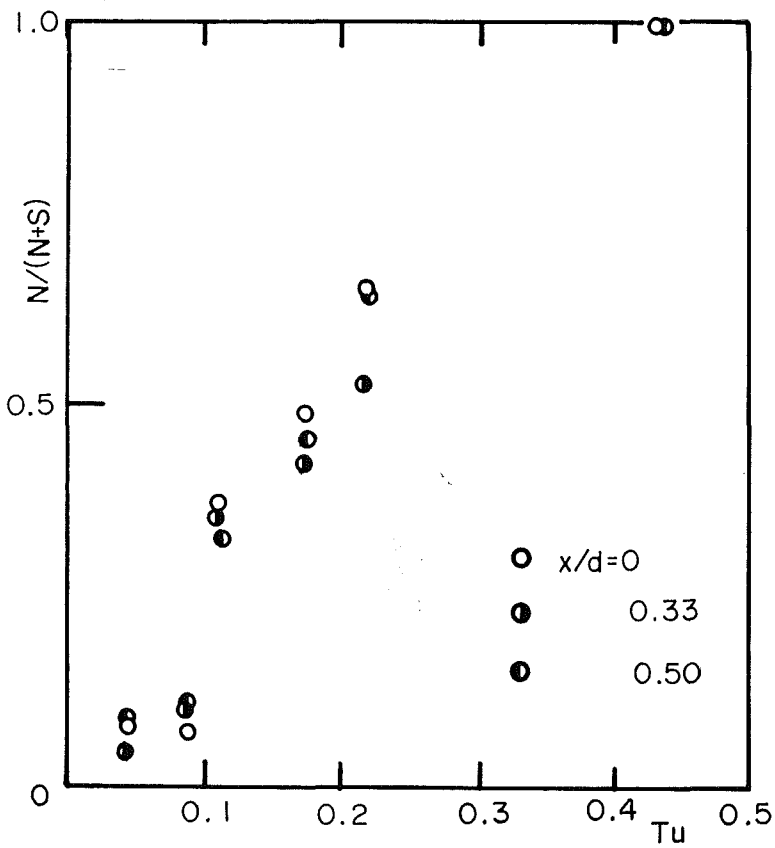

Fig. 9. $N/(N+S)$ versus turbulence parameter Tu.

relation length L_z/d; a minimum appears at $x/d \fallingdotseq 0.5$ and a maximum in the range of $1 \leqq x/d \leqq 2$. From Fig. 8, an important effect of the turbulence scale on the S/N ratio is also clear if one compares the results of cases 1, 2 and 3, i.e. the S/N ratio decreases as L_x/d decreases under the same magnitude of the turbulence intensity. Although a minimum of S/N disappears for cases 3-6, a maximum somewhere in the range $1 \leqq x/d \leqq 2$ still remains to be observed. The results of Figs. 6 and 8 may suggest an alternative definition of the end of the formation region in terms of the spanwise correlation length and the S/N ratio of the energy of the velocity fluctuations. Figure 9 shows the relation between the ratio $N/(N+S)$ and the turbulence parameter Tu for the range $0 \leqq x/d \leqq 0.5$ downstream of the cylinder. It can clearly be seen that the values of $N/(N+S)$ are well correlated with the parameter Tu.

5. Concluding remarks

In the Reynolds-number range of $1.1 \times 10^4 \sim 4.1 \times 10^4$ studied in this paper, the aerodynamic characteristics of a circular cylinder measured in turbulent flow are found to be considerably different from those measured in a smooth flow.

The main results of the present study may be summarized as follows:

1) The base-pressure coefficient C_{pb}, drag coefficient C_D, Strouhal number St, spanwise correlation length $(L_z/d)_{\theta=90°}$ and noise-to-signal ratio defined as $N/(N+S)$ are fairly well correlated with the turbulence parameter $Tu=[(\overline{u'^2})^{1/2}/U_\infty](d/L_x)$, while the parameters suggested by Taylor[4] and Bearman[3] are found to be inappropriate in this respect.

2) The time-averaged drag force acting on a circular cylinder decreases as the turbulence intensity increases. If the turbulence intensity remains constant, the drag force decreases as the nondimensional length scale L_x/d of the turbulence decreases.

3) The spanwise correlation length of shed vortices considerably decreases with an increase of the turbulence intensity and with a decrease of the turbulence-length scale.

4) The ratio S/N decreases with the increase of the turbulence intensity. Definite vortex shedding does not appear for sufficiently large turbulence intensity.

5) The spanwise correlation length L_z and S/N ratio respectively attain maximum values at the end of the formation region of shed vortices.

6) The Strouhal number is rather insensitive to the turbulence intensity in the range where $Tu<0.2$. It slightly increases for the turbulence parameter larger than 0.2.

The present research is supported by a Grant-in-Aid for Scientific Research from the Ministry of Education. The authors express their sincere thanks to Mr. H. Tamura, Instructor of Fluid Mechanics I, for his valuable discussions regarding the experimental results and to Mr. T. Yamazaki and Mr T. Sampo, Techical Officials of the Ministry of Education, for their assistance in constructing the experimental apparatus.

References

1) Hunt, J. C. R.: J. Fluid Mech., 61 (1973), p. 625.
2) Batchelor, G. K. and Proudman, I.: Quart. J. Mech. and Applied Math., 7 (1954), p. 83.
3) Bearman, P. W.: J. Fluid Mech., 46-1 (1971), p. 177.
4) Taylor, G. I.: Proc. Roy. Soc. Lond., A. Vol. CLVI (1937), p. 307.
5) Hinze, J. O.: Turbulence (1959), p. 135, McGraw-Hill.
6) Allen, H. J. and Vincenti, W. G.: N. A. C. A. Wash. Rep. 782 (1944).
7) Bearman, P. W. and Wadcock, A. J.: J. Fluid Mech., 61-3 (1973), p. 499.
8) El Baroudi, M. Y.: U. T. I. A. S. Tech. Note, No. 31 (1960).
9) Bloor, M. S.: J. Fluid Mech., 19-2 (1964), p. 290.
10) Surry, D.: J. Fluid Mech., 52-3 (1972), p. 543.